Liquid Crystals
Publication details, including instructions for authors and subscription information:
http://www.informaworld.com/smpp/title~content=t713926090

Banana-shaped mesogens: effect of lateral substituents on seven-ring esters containing a biphenyl moiety

H. N. Shreenivasa Murthy; B. K. Sadashiva

Online publication date: 11 November 2010

To cite this Article Murthy, H. N. Shreenivasa and Sadashiva, B. K.(2002) 'Banana-shaped mesogens: effect of lateral substituents on seven-ring esters containing a biphenyl moiety', Liquid Crystals, 29: 9, 1223 — 1234
To link to this Article: DOI: 10.1080/02678290210160114
URL: http://dx.doi.org/10.1080/02678290210160114

LIQUID CRYSTALS, 2002, VOL. 29, NO. 9, 1223–1234

Taylor & Francis
Taylor & Francis Group

Banana-shaped mesogens: effect of lateral substituents on seven-ring esters containing a biphenyl moiety

H. N. SHREENIVASA MURTHY and B. K. SADASHIVA*
Raman Research Institute, C.V. Raman Avenue, Sadashivanagar,
Bangalore 560 080, India

(*Received 21 February 2002; accepted 29 April 2002*)

The synthesis and characterization of five homologous series of symmetrical compounds composed of banana-shaped molecules containing a biphenyl moiety are reported. All these compounds are non-Schiff's bases and are esters. The effects of lateral substituents such as fluoro, methyl and ethyl in the side arms of these molecules are examined. These substituents have a strong influence in reducing the clearing temperatures. Banana phases such as B_1, B_2 and B_6 were observed in the above series of compounds. The mesophases were characterized by a combination of polarizing optical microscopy, differential scanning calorimetry, X-ray diffraction and electro-optic studies.

1. Introduction

The discovery of electro-optic switching by the smectic phase of an achiral bent-core compound [1] and the subsequent beautiful demonstration [2] that the switching is actually antiferroelectric in nature have evoked keen interest and paved the way for a new sub-field of liquid crystals, viz. banana-shaped mesogens. During the last few years, many compounds composed of banana-shaped molecules have been synthesized by different groups around the world with a view to investigating the structure, as well as other physical properties of their mesophases [3–13].

So far, at least seven phases have been identified as belonging to this class of compound and given the code letters B_1 to B_7 as agreed upon at a conference in Berlin in 1997 [14]. The B_1 phase has a two-dimensional periodic structure while the B_2 phase is a fluid smectic phase associated with antiferroelectric characteristics. The B_3 and B_4 phases have been shown to be crystalline by X-ray studies, though the B_4 phase shows an intense blue colour [4]. The B_5 phase, which has so far been observed in only three compounds, has the same symmetry as the B_2 phase, but with an additional in-plane order [4]. The B_6 phase, which exhibits a fan-shaped texture, is well understood and the available data are indicative of an intercalated structure [4]. The B_7 phase shows extraordinary textures not seen for any of the other B phases; its structure is not clear and appears to be somewhat complicated. Further, from results being reported in the literature, it is clear that the addition of new mesophases to this list is likely with the passage of time.

*Author for correspondence; e-mail: sadashiv@rri.res.in

In order to understand the relationship between the molecular structure of banana-shaped compounds and the mesophases they exhibit, a systematic examination of a large number of compounds is necessary. The study of the influence of lateral substituents in the arms of such compounds is an important exercise in this direction. The influence of lateral substituents on the mesophase behaviour of several members of seven new series of bent-shaped five-ring resorcinol derivatives was examined recently by Weissflog *et al.* [15]. In this study, the central phenylene unit was substituted with fluorine, chlorine, methyl, cyano or nitro groups, as well as with two chloro substituents. Also fluorine, chlorine, methyl and trifluormethyl substituents were attached at the outer aromatic rings. In an earlier communication [16], we reported the effect of some lateral substituents in the middle phenyl ring on the mesophases formed by these bent-core compounds. In this paper, we report the synthesis of five different homologous series of compounds, the characterization of their mesophases, as well as the effect of lateral substituents in more detail. We have chosen a seven-ring system containing a biphenyl moiety at the ends of the arms of the compounds, since the laterally unsubstituted parent derivatives have fairly wide temperature ranges of the mesophases.

2. Synthesis

All the banana-shaped mesogens (**v**) reported here were synthesized following the general pathway shown in figure 1. The commercially available resorcinol (**i**) was used as obtained. 4-Benzyloxybenzoic acid (**ii**, $X = Y = H$), 2-fluoro-4-benzyloxybenzoic acid (**ii**, $X = F$, $Y = H$) and 3-fluoro-4-benzyloxybenzoic acid (**ii**, $X = H$, $Y = F$) were

Liquid Crystals ISSN 0267-8292 print/ISSN 1366-5855 online © 2002 Taylor & Francis Ltd
http://www.tandf.co.uk/journals
DOI: 10.1080/02678290210160114

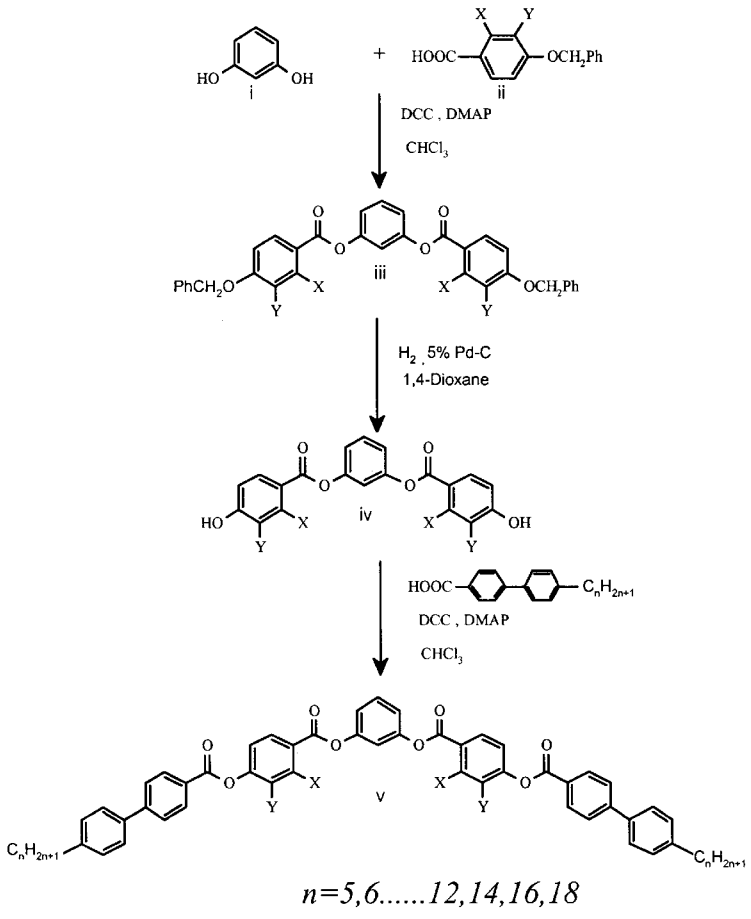

X=H,	Y=H	Series I
X=F ,	Y=H	Series II
$X=CH_3$,	Y=H	Series III
$X=C_2H_5$,	Y=H	Series IV
X=H,	Y=F	Series V

Figure 1. Synthetic pathway used to obtain the banana-shaped mesogens.

prepared following procedures used by us previously [17]. 2-Methyl-4-benzyloxybenzoic acid (**ii**, $X = CH_3$, $Y = H$) and 2-ethyl-4-benzyloxybenzoic acid (**ii**, $X = C_2H_5$, $Y = H$) were prepared from *m*-cresol and *m*-ethylphenol, respectively, following a procedure similar to that described by us earlier [18]. 4-*n*-Alkylbiphenyl-4′-carboxylic acids were prepared as described previously [19]. The detailed procedure for one of the target compounds, **30**, is outlined below.

2.1. *1,3-Phenylene bis(2-methyl-4-benzyloxybenzoate),* ***iii*** *($X = CH_3$, $Y = H$)*

A mixture of resorcinol (2.27 g, 0.02 mol), 2-methyl-4-benzyloxybenozic acid (10 g, 0.04 mol) and 4-*N*,*N*-dimethylaminopyridine (DMAP) (0.5 g, 0.004 mol) in dry chloroform (50 ml) was stirred for 10 min. To this was added *N*,*N*′-dicyclohexylcarbodiimide (DCC) (9.05 g, 0.044 mol) and the mixture stirred for 10 h at room temperature. The *N*,*N*′-dicyclohexylurea formed was filtered off and washed with chloroform (15 ml). The combined filtrate was washed with 5% aqueous acetic acid (2 × 50 ml), 5% aqueous sodium hydroxide (2 × 50 ml) and water (3 × 50 ml) and dried over anhydrous sodium sulphate. The solvent was removed from the solution, yielding a white residue. This was chromatographed on silica gel using chloroform as eluent and the white material obtained after evaporating the solvent was crystallized from acetonitrile. Yield 9.0 g (78%), m.p. 128–129°C. IR ν_{max} (nujol): 1720, 1605, 1225 and 1120 cm^{-1}. ^1H NMR ($CDCl_3$) δ: 2.66 (s, 6H,

2 × Ar–CH_3), 6.89 (d, J 7.2 Hz, 2H, Ar–H), 7.11 (d, J 7.2 Hz, 2H, Ar–H), 7.33–7.48 (m, 14H, Ar–H), 8.17 (d, J 9.6 Hz, 2H, Ar–H). $C_{36}H_{30}O_6$ requires C 77.40, H 5.41; found C 76.98, H 5.34%.

2.2. *1,3-Phenylene bis(2-methyl-4-hydroxybenzoate), iv (X = CH_3, Y = H)*

A mixture of compound **iii** (8.5 g, 0.015 mol), 5% Pd-C catalyst (2.0 g) and 1,4-dioxane (150 ml) was stirred at 50°C in an atmosphere of hydrogen until the calculated quantity of hydrogen was absorbed. The reaction mixture was filtered and removal of solvent from the filtrate gave a residue which was crystallized from a mixture of 1,4-dioxane and petroleum ether (b.p. 60–80°C). Yield 6.0 g (85%), m.p >255°C (dec). IR ν_{max} (nujol): 3380, 1700, 1605, 1220 and 1120 cm^{-1}. ^1H NMR ($CDCl_3$) δ: 2.40 (s, 6H, 2 × Ar–CH_3), 9.8 (s, 2H, 2 × Ar–OH), 7.12 (d, J 8.4 Hz, 2H, Ar–H), 7.3–7.33 (m, 3H, Ar–H), 7.64 (t, J 8.4 Hz, 1H, Ar–H), 8.0–8.07 (m, 4H, Ar–H). $C_{22}H_{18}O_6$ requires C 69.83, H 4.80; found C 69.38, H 4.71%.

2.3. *1,3-Phenylene bis[4-(4′-n-dodecylbiphenyl-4-carbonyloxy)-2-methylbenzoate], 30*

A mixture of compound **iv** (0.19 g, 0.0005 mol), 4′-*n*-dodecylbiphenyl-4-carboxylic acid (0.37 g, 0.001 mol), DMAP (0.012 g,) and dry chloroform (10 ml) was stirred for 5 min. To this was added DCC (0.226 g, 0.0011 mol) and the mixture stirred overnight at room temperature. The precipitated N,N'-dicyclohexylurea was filtered off and washed with chloroform (5 ml). The combined filtrate was washed with 5% aqueous acetic acid (2 × 20 ml), 5% ice-cold aqueous sodium hydroxide (2 × 20 ml) and water (3 × 25 ml) and dried over anhydrous sodium sulphate. Removal of the solvent after filtration gave a white residue, which was chromatographed on silica gel using chloroform as eluent. Removal of solvent from the eluate gave the required compound which was crystallized from a mixture of chloroform and acetonitrile. Yield 0.35 g (70%), m.p 115°C. IR ν_{max} (nujol): 1725, 1600, 1460, 1220 cm^{-1}. ^1H NMR ($CDCl_3$) δ: 0.87–0.9 (t, 6H, 2 × $-CH_3$), 1.21–1.66 (m, 40H, 20 × $-CH_2-$), 2.65–2.69 (t, J 7.7 Hz, 4H, 2 × Ar–CH_2-), 2.73 (s, 6H, 2 × Ar–CH_3), 7.17–7.3 (m, 11H, Ar–H), 7.50 (t, J 8.2 Hz, 1H, Ar–H), 7.58 (d, J 8.2 Hz, 4H, Ar–H), 7.74 (d, J 8.2 Hz, 4H, Ar–H), 8.24–8.30 (m, 6H, Ar–H). $C_{72}H_{82}O_8$ requires C 80.41, H 7.69; found C 80.25, H 7.91%.

In general, all intermediate compounds as well as final materials were purified by chromatographic techniques and by repeated crystallization from suitable solvents. The purity of all the compounds was checked by thin layer chromatography (Merck kieselgel $60F_{254}$ precoated plates) as well as by high performance liquid chromatography (μ porasil column 3.9 mm × 300 mm, Waters Associates Inc.) using 1% ethyl acetate in dichloromethane as the eluent. The yields of compounds were in the range 65–85%.

3. Characterization

The chemical structures of all the compounds were confirmed by using a combination ^1H NMR spectroscopy (Bruker AMX 400 spectrometer) with 1% tetramethylsilane in deuteriochloroform as an internal standard, infrared spectroscopy (Shimadzu FTIR-8400 spectrophotometer) and elemental analysis (Carlo-Erba 1106 analyser). The thermal phase behaviour of all the homologous series of compounds was examined by using polarizing optical microscopy (POM) (Leitz Laborlux 12POL/Olympus BX50) in conjunction with a heating stage and controller (Mettler FP 52 and FP5, respectively) and also from thermograms recorded by differential scanning calorimetry (DSC) (Perkin-Elmer, Model Pyris 1D). The enthalpies for the various transitions were also determined using DSC, the calorimeter having been calibrated using pure indium as standard. The phase identification was made by observation of the optical textures and the mesophase structure was confirmed by X-ray diffraction (XRD) studies using CuK_α radiation from a rotating anode generator (Rigaku Ultrax 18) with a flat graphite crystal monochromator. The diffraction patterns were collected on an image plate (Marresearch). Unoriented samples were contained in Lindemann capillaries and the sample temperature in each case was controlled to within ±0.1°C. The electro-optical studies were performed employing a standard experimental set-up wherein the sample was mounted between ITO-coated homogeneously aligned glass plates and viewed by POM. The switching current response was obtained using the triangular voltage method.

4. Results and discussion

In order to assess the effect of lateral substituents on the mesophases of these banana-shaped compounds, it would be useful, initially, to look at the trends in the mesomorphic behaviour of the unsubstitued parent compounds, particularly along a homologous series. Obviously several series of compounds have to be evaluated before any general conclusions can be drawn about the effect of substituents. Here, we examine the effect of lateral substituents such as methyl, ethyl and fluoro comprising four series as outlined below. The transition temperatures and the associated enthalpies of transition for the unsubstituted parent compounds are summarized in table 1. The mesomorphic properties of some of the compounds of this series were reported [16]

Table 1. Transition temperatures (°C) and enthalpies (kJ mol^{-1}) (*in italics*) for the compounds of series I.

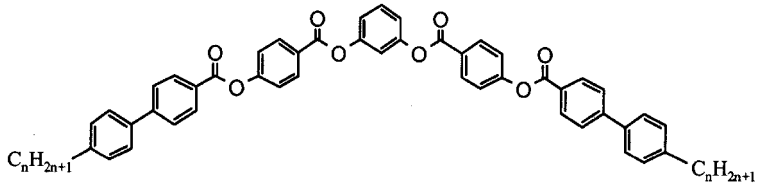

Key for tables 1–5: Cr = Crystalline phase; B1 = two-dimensional banana phase; B2 = lamellar antiferroelectric banana phase; B6 = intercalated smectic banana phase; I = isotropic phase; (nomenclature as adopted at the International Workshop on Banana-Shaped Liquid Crystals: Chirality by Achiral Molecules' held in Berlin, December 1997).

Compound	*n*	Cr		B2		B1		B6		I
1	5	•	175.0 *36.22*	—		•	246.0 *0.41*	•	257.0 *18.79*	•
2	6	•	165.0 *39.55*	—		•	240.0 *23.62*	—		•
3	7	•	163.5[a] *50.56*	—		•	235.0 *23.46*	—		•
4	8	•	153.5 *36.14*	—		•	226.0 *23.81*	—		•
5	9	•	141.0 *50.98*	—		•	219.0 *24.24*	—		•
6	10	•	159.0 *42.87*	—		•	211.0 *23.76*	—		•
7	11	•	151.0[a] *61.42*	•	209.0 *25.45*	—		—		•
8	12	•	121.0[a] *53.14*	•	209.0 *26.98*	—		—		•
9	14	•	118.0 *45.05*	•	208.5 *27.67*	—		—		•
10	16	•	117.5 *43.78*	•	206.5 *28.72*	—		—		•
11	18	•	117.0 *48.05*	•	204.0 *28.47*	—		—		•

[a] Has a crystal–crystal transition and the enthalpy denoted is the sum for all transitions.

earlier. As can be seen, only one compound (**1**) shows the B6 phase with the characteristic fan-shaped texture and a thermal range of 11°C. This compound, as well as compounds **2** to **6**, exhibits the two-dimensional B1 phase. The nature of the phase has been confirmed by X-ray studies as shown for compound **5** [16]. Compounds **7** to **11** show the antiferroelectric B2 phase, which has been confirmed by X-ray as well as by its electro-optical switching characteristics [16]. All the compounds of this series have high clearing temperatures (>200°C) and fairly wide thermal ranges for the B1 and B2 phases which facilitate the study of the effect of lateral substituents. A plot of the transition temperatures as a function of the length of the terminal alkyl chain is shown in figure 2. One can see that the B1 to isotropic temperatures fall on ascending the series and these points fall on a smooth curve. The B2 to isotropic transition points also fall on a smooth curve which is similar to that observed for such transitions previously [13].

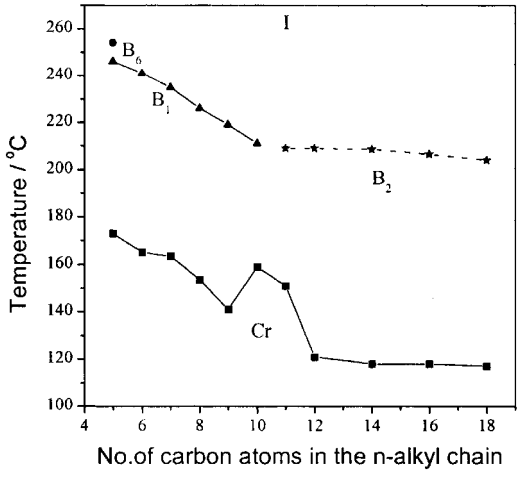

Figure 2. Plot of transition temperatures vs the number of carbon atoms in the *n*-alkyl chain of the compounds of series I.

It is very interesting to note that compounds **9**, **10** and **11** exhibit optical textures different from those of compounds **7** and **8**. On slow cooling of the isotropic liquid of compound **9**, small fractal domains appear and coalesce on further cooling to give a grainy texture. Typical textures observed for these three compounds are shown in figure 3 for compound **9**. While observing these textures one can clearly distinguish two domains when the polarizer and the analyser are crossed. When the analyser is rotated by 5°, one can see some domains appearing bright; by rotating the analyser in the opposite direction by the same number of degrees from the original position, these domains become slightly darker. This clearly indicates that there are two regions in the same sample having opposite handedness. Similar textures have been observed previously by Heppke *et al.* [8] and Thisayukta *et al.* [20, 21]. While the sulphur-containing compounds show switching behaviour [8], those susbsituted by a central naphthylene unit are smectic and switching characteristics have not been reported. The X-ray data for our compounds point to a lamellar order and electro-optical studies show that they are antiferroelectric in nature. In addition, it can be seen that the clearing temperatures of these three compounds follow the curve (figure 2) for the B_2 to isotropic transition points. These results indicate that although the texture is different from that normally seen for the B_2 phase, the mesophase of these three compounds can be classified as B_2.

The transition temperatures together with the associated enthalpies of transition for the compounds of series II ($X = F$, $Y = H$) are collected in table 2. The effect of the fluoro substituent, which is *ortho*- to the carbonyl group, on the mesophases is rather interesting. All the three mesophases observed in the parent compounds are retained, but the melting and clearing temperatures are reduced in every case. While the temperature range of the B_6 phase has been reduced from 11°C to 2°C (compounds **1** and **12**), the ranges for the B_1 and B_2 phases are increased. Compound **6** exhibits a B_1 phase while the corresponding fluoro substituted compound **17** shows a B_2 phase with a thermal range of 80°C. A plot of the transition temperatures against the number of carbon atoms in the alkyl chain for the compounds of series II is shown in figure 4. Here also one can see the clearing transitions falling on two curves, one for the B_1 phase and the other for the B_2 phase. The slopes of the two curves are very similar to those observed for the homologues of series I.

As observed in series I, compounds **20**, **21** and **22** exhibit a grainy texture forming from domains of opposite handedness as described earlier. For the same reasons given earlier, we have designated the mesophase of these three compounds as B_2.

In table 3, the transition temperatures and associated enthalpies for the compounds of series III are summarized. The effect of the lateral methyl group, which is

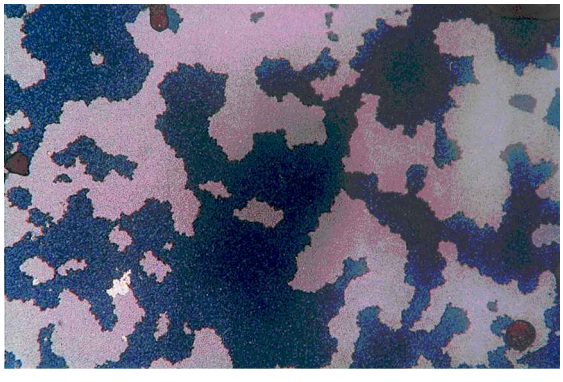

(*a*)

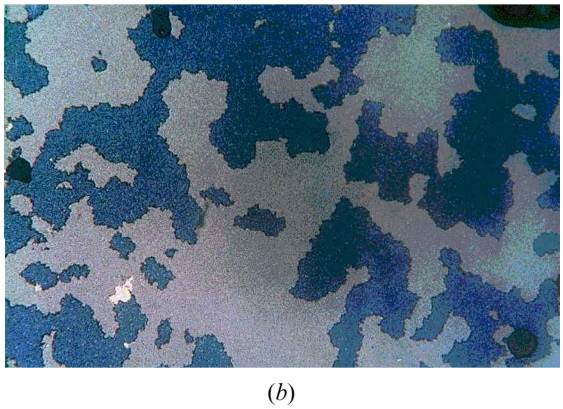

(*b*)

Figure 3. (*a*) Photomicrograph of the texture of compound **9** obtained at 203°C, magnification ×200; (*b*) the same area obtained after rotating the analyser by 5°.

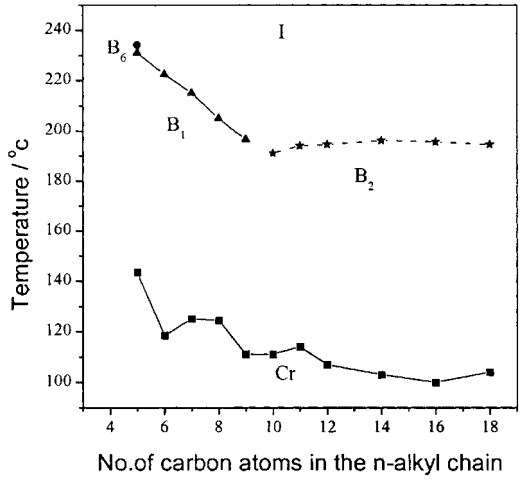

Figure 4. Plot of transition temperature vs the number of carbon atoms in the *n*-alkyl chain of the compounds of series II.

Table 2. Transition temperatures (°C) and enthalpies (kJ mol^{-1}) (*in italics*) for the compounds of series II.

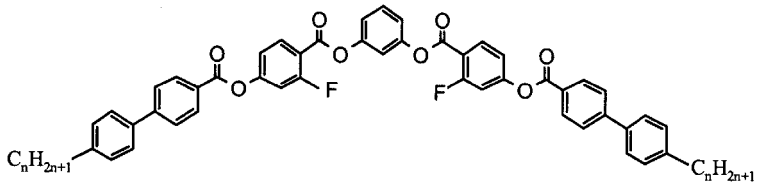

Compound	n	Cr		B_2		B_1		B_6	I
12	5	•	143.5	—	•	232.0	•	234.0	•
			29.61			*0.02*		*16.87*	
13	6	•	134.0	—	•	222.5	—		•
			37.55			*21.58*			
14	7	•	125.0	—	•	215.0	—		•
			29.71			*22.46*			
15	8	•	124.5	—	•	205.0	—		•
			29.78			*22.57*			
16	9	•	110.0	—	•	196.5	—		•
			28.21			*21.49*			
17	10	•	111.0	•	191.0	—	—		•
			29.23		*22.9*				
18	11	•	114.0	•	194.0	—	—		•
			31.78		*22.96*				
19	12	•	107.0	•	194.5	—	—		•
			50.36		*22.46*				
20	14	•	103.0	•	196.0	—	—		•
			72.55		*27.67*				
21	16	•	100.0	•	195.5	—	—		•
			85.09		*29.03*				
22	18	•	104.0	•	194.5	—	—		•
			73.96		*29.92*				

ortho- to the carbonyl group, can be seen here. There is a general reduction in the melting and clearing points as compared with the unsubstituted compounds. In addition, the B_1 phase of compounds **2** and **3** is suppressed and the B_6 phase is induced in compounds **24** and **25**. A typical texture of the B_1 phase growing from the isotropic phase is shown in figure 5. The antiferroelectric B_2 phase commences for the homologue with $n = 12$ (compound **30**); this phase appeared for compound **7** (with $n = 11$) in series I. A plot of the melting and clearing temperatures against the number of carbon atoms in the alkyl chain for compounds of this series is shown in figure 6. Again, it can be seen that the clearing transitions involving the three phases B_6, B_1 and B_2 lie on smooth curves.

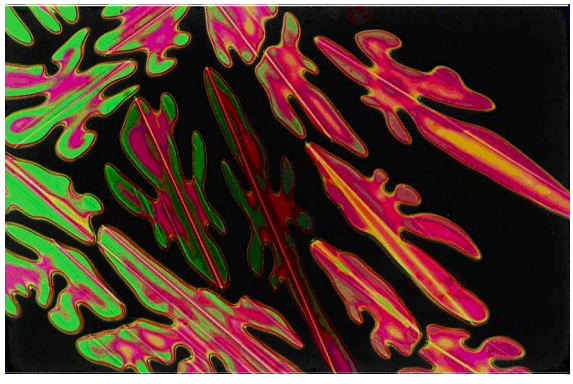

Figure 5. Photomicrograph of the texture growing from the isotropic phase of compound **29** at 156°C, magnification ×200.

In order to see the effect of a slightly larger group, we introduced an ethyl group in place of the methyl group (series IV). The transition temperatures and the corresponding enthalpies for these compounds **34** to **44** are collected in table 4. As before, there is a reduction in the melting points, while the clearing temperatures are suppressed drastically. More interestingly, the existence of the B_6 phase is enhanced while that of the B_1 and the B_2 phases is suppressed. For, example, compound **1** has a thermal range of 11°C for the B_6 phase and compounds **1** to **6** show a fairly wide thermal range for the B_1 phase (>52°C). In contrast, the analogous ethyl-substituted compounds **34** to **38** show a B_6 phase, while the B_1 phase is completely eliminated for these compounds. Similarly compounds **7** to **11** show wide thermal ranges (58 to 90°C) for the B_2 phase, while the analogous

Table 3. Transition temperatures (°C) and enthalpies (kJ mol^{-1}) (*in italics*) for the compounds of series III.

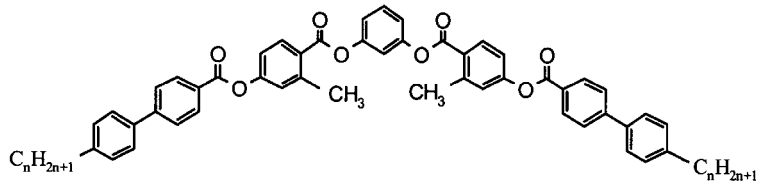

Compound	*n*	Cr		B2		B1		B6		I
23	5	•	143.0[a]	—		(•	127.0)	•	201.0	•
			52.33				*0.02*		*13.43*	
24	6	•	143.5[a]	—		•	155.0	•	190.0	•
			43.32				*0.11*		*14.54*	
25	7	•	118.5	—		•	175.0	•	182.0	•
			30.91				*0.12*		*15.63*	
26	8	•	104.0	—		•	172.0	—		•
			27.96				*18.67*			
27	9	•	101.0	—		•	167.5	—		•
			24.83				*19.87*			
28	10	•	119.5[a]	—		•	162.0	—		•
			39.59				*19.89*			
29	11	•	112.5	—		•	157.0	—		•
			40.53				*21.58*			
30	12	•	115.0[a]	•	154.5	—		—		•
			61.94		*23.10*					
31	14	•	103.0	•	156.5	—		—		•
			28.63		*24.18*					
32	16	•	103.5[a]	•	156.0	—		—		•
			74.06		*25.03*					
33	18	•	103.0	•	155.0	—		—		•
			84.80		*24.18*					

[a] Has a crystal–crystal transition and the enthalpy denoted is the sum for the transitions.

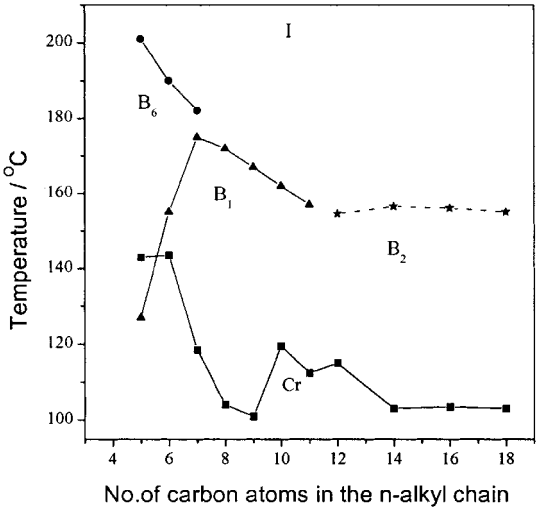

Figure 6. Plot of transition temperatures vs the number of carbon atoms in the *n*-alkyl chain of the compounds of series III.

ethyl-substituted compounds **40** and **41** show a metastable B1 phase, and compounds **42** to **44** exhibit metastable B2 phases. Thus, the ethyl group destabilizes the B1 and B2 phases while stabilizing the B6 phase for the higher alkyl chain (upto $n = 9$). A plot of the transition temperatures as a function of the terminal alkyl chain length for this series is shown in figure 7. The slope for the B6 to isotropic transition curve is quite steep. Three homologues each of this series show the B1 and B2 phases and the clearing temperatures for these phases lie on curves which are typical for such transitions.

The transition temperatures and the associated enthalpies for compounds of series V are summarized in table 5. In this series, the fluoro substituent is in the *meta*- position with respect to the carbonyl group. We had earlier reported [16] on the mesophases of three homologues of this series, which show the two-dimensional B1 phase. It is interesting to note that as in the previous three series of compounds, there is a suppression of the clearing temperatures, but in contrast the melting points increase for four homologues (compounds **52** to **55**). While the existence of the B6 phase is unaffected, the smectic B2 phase is eliminated in two of the compounds (**51** and **52**) as compared with the parent analogues, and the occurrence of the B1 phase is enhanced as eight of the eleven homologues show this

Table 4. Transition temperatures (°C) and enthalpies (kJ mol^{-1}) (*in italics*) for the compounds of series IV.

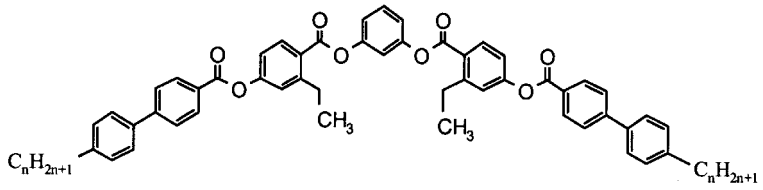

Compound	*n*	Cr		B_2		B_1		B_6		I
34	5	●	132.0 *40.63*	—		—		●	142.5 *9.95*	●
35	6	●	129.0 *32.55*	—		—		●	133.0 *10.20*	●
36	7	●	113.0 *30.05*	—		—		●	128.5 *11.41*	●
37	8	●	99.0[a] *27.55*	—		—		●	118.5 *11.29*	●
38	9	●	102.5 *36.70*	—		—		●	112.5 *12.34*	●
39	10	●	104.5 *36.03*	—		●	106.0 *12.75*	—		●
40	11	●	105.5[a] *56.50*	—		(●	103.0) *13.90*	—		●
41	12	●	104.5 *56.05*	—		(●	99.0) *15.42*	—		●
42	14	●	105.0 *58.53*	(●	94.0) *18.90*	—		—		●
43	16	●	104.5 *58.34*	(●	96.5) *15.13*	—		—		●
44	18	●	104.0 *67.45*	(●	98.5) *21.28*	—		—		●

[a] Has a crystal–crystal transition and the enthalpy denoted is the sum for the transitions.

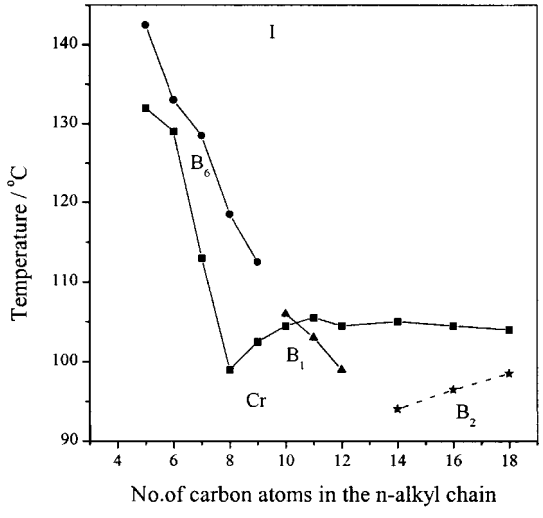

Figure 7. Plot of transition temperatures vs the number of carbon atoms in the *n*-alkyl chain of the compounds of series IV.

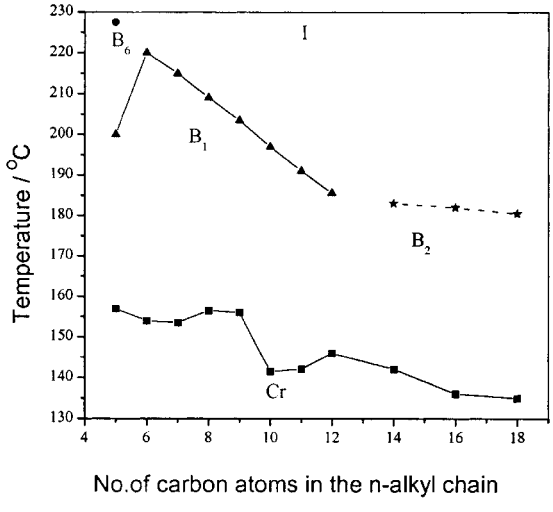

Figure 8. Plot of transition temperatures vs the number of carbon atoms in the *n*-alkyl chain of the compounds of series IV.

phase. As was shown previously [16], on substitution in the *meta*- position by groups which either donate or withdraw electrons in this type of system, the layered mesophase is suppressed more. A plot of the transition temperatures as a function of the *n*-alkyl chain length is shown in figure 8. As usual, the curves for the clearing

Table 5. Transition temperatures (°C) and enthalpies (kJ mol^{-1}) (*in italics*) for compounds of series V.

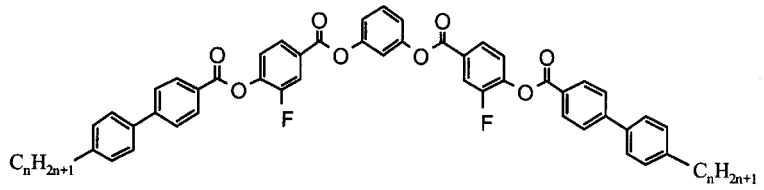

Compound	*n*	Cr		B_2		B_1		B_6		I
45	5	•	157.0	—		•	200.0	•	227.5	•
			32.59				*0.41*		*15.0*	
46	6	•	154.0	—		•	220.0	—		•
			23.28				*19.58*			
47	7	•	153.5	—		•	215.0	—		•
			21.08				*20.90*			
48	8	•	156.5	—		•	209.0	—		•
			56.74				*22.12*			
49	9	•	156.0	—		•	203.5	—		•
			57.54				*22.21*			
50	10	•	141.5	—		•	197.0	—		•
			27.96				*22.70*			
51	11	•	142.0	—		•	191.0	—		•
			35.86				*22.13*			
52	12	•	146.0	—		•	185.5	—		•
			40.04				*22.07*			
53	14	•	142.0	•	183.0	—		—		•
			47.36		*23.79*					
54	16	•	136.0[a]	•	182.0	—		—		•
			49.15		*21.27*					
55	18	•	135.0	•	180.5	—		—		•
			57.35		*24.20*					

[a] Has a crystal–crystal transition and the enthalpy denoted is the sum for the transitions.

temperatures of the B_1 and B_2 phases show the trends seen previously.

The effects for the *ortho*- and *meta*-fluoro substituted compounds (series II and V) may be summed up as follows. All the compounds of series V have higher melting points while the clearing temperatures are lowered generally, except for compounds **48**, **49** and **50**. However, the existence of the lamellar B_2 phase seems to be favoured in the *ortho*-substituted derivatives. It is also interesting to note that the *meta*-substituted chloro compounds [12] and the corresponding fluoro analogues behave similarly along the series. In contrast however, the *ortho*- and *meta*-substituted methyl derivatives show a different behaviour. The former derivatives (series III) exhibit the B_6, B_1 and B_2 mesophases over an extended range of temperature and the melting points are suppressed, while the clearing temperatures are higher.

5. X-ray diffraction studies

From the optical textures, we have identified three mesophases, B_6, B_1 and B_2, which are present in all five series of compounds. The nature of these phases has been confirmed by XRD studies of unoriented samples. The XRD pattern of compound **24** at 180°C shows a diffuse peak in the wide angle region with a spacing of about 4.8 Å which is indicative of liquid-like in-plane order. In the small angle region, two peaks are observed, in the ratio 1 : 2, indicating a lamellar ordering. The *d*-value corresponding to the first reflection in this region is 22.9 Å, which is about half the molecular length. The molecular length was measured by assuming the *n*-alkyl chain to be extended in an all-*trans*-conformation. This suggests an intercalated structure of the mesophase as reported by Shen *et al.* [22] and Pelzl *et al.* [4]. A typical X-ray intensity profile of the mesophase of compound **24** at 180°C is shown in figure 9. This mesophase with a focal-conic texture has been identified as a B_6 phase.

The XRD pattern of an unoriented sample of compound **29** shows three reflections in the small angle region with $d_1 = 35.5$ Å, $d_2 = 26.1$ Å and $d_3 = 15.8$ Å, which can be indexed as (1 1), (0 2) and (3 1) reflections of a two-dimensional rectangular lattice. The lattice parameters are $a = 48.6$ Å and $b = 52.1$ Å. From the

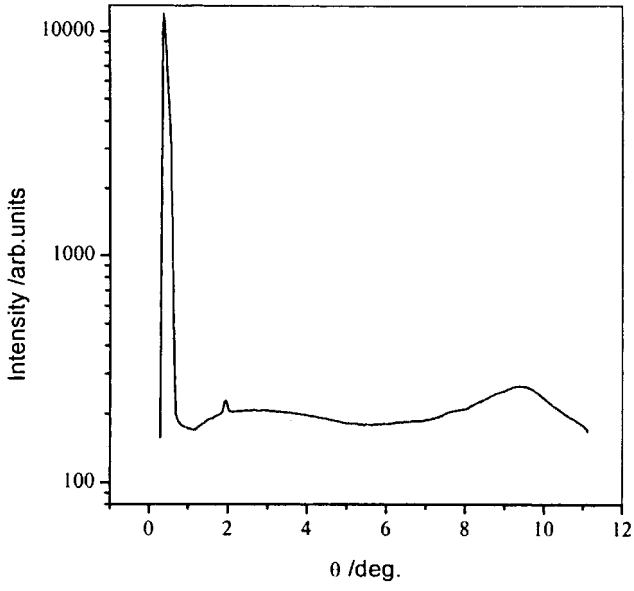

Figure 9. X-ray intensity profile of an unoriented sample of compound **24** at 180°C.

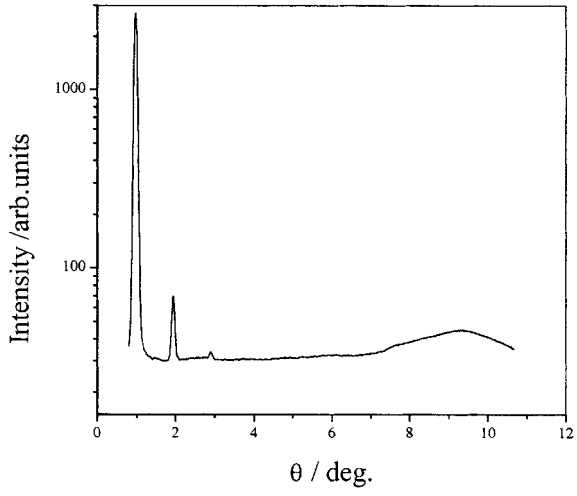

Figure 11. X-ray intensity profile of an unoriented sample of compound **30** at 140°C.

mosaic texture coupled with the XRD data, this phase has been designated as a B_1 mesophase. The X-ray intensity profile for this phase is shown in figure 10.

The diffraction pattern obtained for compound **30** at 140°C shows three reflections in the small angle region with d-values of 45.5, 22.8 and 15.2 Å. These are in the ratio 1:2:3 which is typical for lamellar ordering. The tilt of the molecules has been estimated to be about 46°. The diffuse wide angle reflection at about 4.6 Å is due to the mobility of the alkyl chains. An X-ray angular intensity profile of this phase at 140°C for compound **30** is given in figure 11. Based on the optical texture exhibited by this compound, the XRD patterns and, as we shall see in the next section, the electro-optical behaviour, this mesophase has been identified as a B_2 phase.

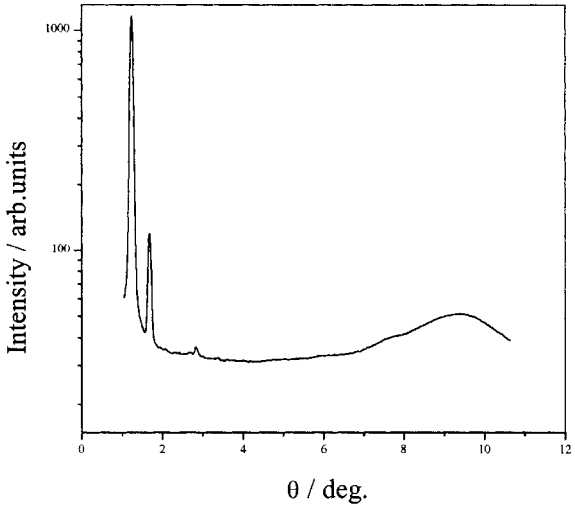

Figure 10. X-ray intensity profile of an unoriented sample of compound **29** at 150°C.

6. Electro-optical studies

The effect of a d.c. electric field on the mesophase of compound **30** has been established. To carry out this study, the sample was taken in a cell of 11 μm thickness, constructed from conducting glass plates coated with polyimide and rubbed for homogeneous alignment. The sample was introduced in the isotropic phase, cooled slowly, and simultaneously viewed between crossed polarizers under a polarizing microscope. On applying a field of 30 V, colourful spherulites started to appear and stabilized around 35 V. The orientation of the brushes changes on reversing the polarity of the applied field. On switching off the field, the dark brushes reorient along the direction of the crossed polarizers. The changes in the rotation of the brushes due to the applied field for compound **30** at 150°C are shown in figure 12. This type of behaviour is typical for the B_2 phase.

To confirm the antiferroelectric switching behaviour of this phase, we carried out polarization measurements using the triangular wave method. A cell of 10 μm thickness was constructed for homogenous alignment, and a sample of compound **30** was introduced in the isotropic phase and cooled slowly. As the transition to the mesophase took place, the applied field was increased gradually to obtain good alignment. By applying a sufficiently high (220 V_{PP} at 15 Hz) triangular voltage, two current peaks per half cycle could be seen on the oscilloscope screen. A typical switching current response obtained for this compound is shown in figure 13. The apparent 'saturated polarization' $\mathbf{P}_S$ was calculated from

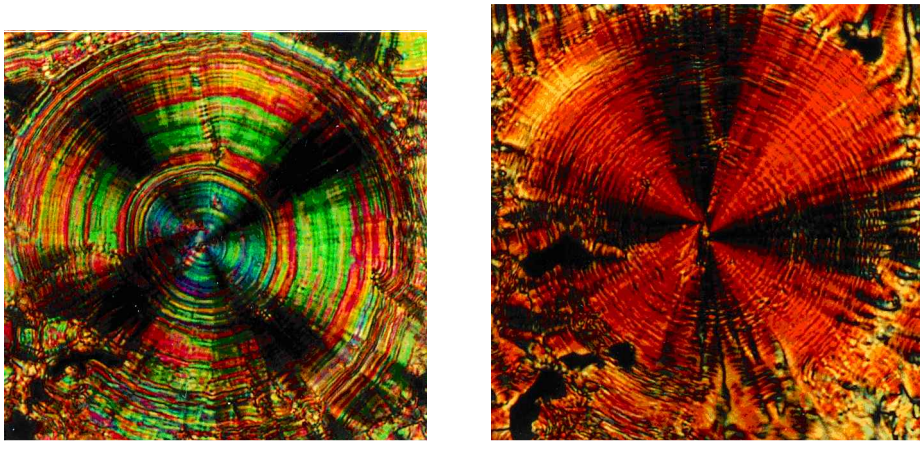

(*a*) (*b*)

(*c*)

Figure 12. Photomicrographs illustrating the effect of a d.c. electric field on compound **30** mounted between rubbed polyimide-coated plates at 150°C. Crossed polarizers × 200; (*a*) $E = +35$ V, (*b*) $E = 0$ V, (*c*) $E = -35$ V. Cell thickness, 11 μm.

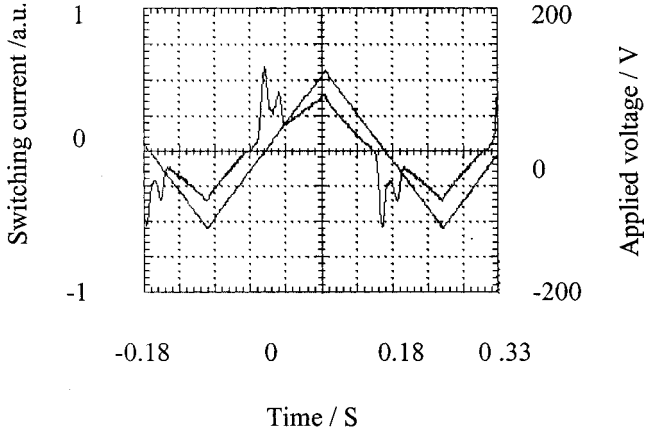

Figure 13. Switching current response obtained for the mesophase of compound **30** by applying a triangular voltage (220 V_{PP}, 15 Hz), sample thickness 10 μm, temperature 150°C. Polarization $\mathbf{P}_S$ 350 nC cm^{-2}.

the area under the peaks and is about 350 nC cm^{-2}. This clearly indicates that the mesophase under investigation is antiferroelectric in nature. Therefore, we can conclude from these studies that the mesophase is indeed B_2.

7. Conclusions

These results indicate that lateral substituents on the arms of these bent-core mesogens generally depress the melting as well as the clearing temperatures. The larger ethyl substituent has a greater effect in depressing the clearing temperature and suppressing the occurrence of a layered mesophase such as B_2, while enhancing the existence of the B_6 phase. It is also found that the *ortho*-fluoro substituted compounds give rise to wide thermal ranges of the B_1 and B_2 mesophases, as compared with the *meta*-substituted analogues. Interestingly compounds

9, **10**, **11**, **20**, **21** and **22** exhibit a sandy or grainy texture with domains of opposite handedness and are all monomesomorphic.

The authors thank Dr V. A. Raghunathan for help in the X-ray measurements, and Ms K. N. Vasudha for technical support. They also wish to thank the Sophisticated Instruments Facility, Indian Institute of Science, Bangalore, where the NMR spectra were recorded.

References

[1] Niori, T., Sekine, T., Watanabe, J., Furukawa, T., and Takezoe, H., 1996, *J. mater. Chem.*, **6,** 1231.
[2] Link, D. R., Natale, G., Shao, R., Maclennan, J. E., Korblova, N. A., and Walba, D. M., 1997, *Science*, **278,** 1924.
[3] Sekine, T., Niori, T., Sone, M., Watanabe, J., Choi, S. W., Takanashi, Y., and Takezoe, H., 1997, *Jpn. J. appl. Phys.*, **36,** 6455.
[4] Pelzl, G., Diele, S., and Weissflog, W., 1999, *Adv. Mater.*, **11,** 707.
[5] Pelzl, G., Diele, S., Jakli, A., Lischka, Ch., Wirth, I., and Weissflog, W., 1999, *Liq. Cryst.*, **26,** 135.
[6] Bedel, J. P., Nguyen, H. T., Rouillon, J. C., Marcerou, J. P., Sigaud, G., and Barois, P., 1999, *Mol. Cryst. liq. Cryst.*, **332,** 163.
[7] Bedel, J. P., Rouillon, J. C., Marcerou, J. P., Laguerre, M., Achard, M. F., and Nguyen, H. T., 2000, *Liq. Cryst.*, **27,** 103.
[8] Heppke, G., Parghi, D. D., and Sawade, H., 2000, *Liq. Cryst.*, **27,** 313.
[9] Weissflog, W., Kovalenko, L., Wirth, I., Diele, S., Pelzl, G., Schmalfuss, H., and Kresse, H., 2000, *Liq. Cryst.*, **27,** 677.
[10] Shen, D., Pegenau, A., Diele, S., Wirth, I., and Tschierske, C., 2000, *J. Am. chem. Soc.*, **122,** 1593.
[11] Sadashiva, B. K., 1999, *Pramana*, **53,** 213.
[12] Sadashiva, B. K., Raghunathan, V. A., and Pratibha, R., 2000, *Ferroelectrics*, **243,** 249.
[13] Amaranatha Reddy, R., and Sadashiva, B. K., 2000, *Liq. Cryst.*, **27,** 1613.
[14] Workshop on *Banana-shaped Liquid Crystals: Chirality by Achiral Molecules*, 1997, Berlin, Germany.
[15] Weissflog, W., Nadasi, H., Dunemann, U., Pelzl, G., Diele, S., Eremin, A., and Kresse, H., 2001. *J. mater. Chem.*, **11,** 2748.
[16] Sadashiva, B. K., Shreenivasa Murthy, H. N., and Dhara, S., 2001, *Liq. Cryst.*, **28,** 483.
[17] Kasthuraiah, N., Sadashiva, B. K., Krishna Prasad, S., and Nair, G. G., 1997, *Liq. Cryst.*, **24,** 639.
[18] Sadashiva, B. K., 1979, *Mol. Cryst. liq. Cryst.*, **53,** 253.
[19] Sadashiva, B. K., and Subba Rao, G. S. R., 1977, *Mol. Cryst. liq. Cryst.*, **38,** 703.
[20] Thisayukta, J., Nakayama, Y., and Watanabe, J., 2000, *Liq. Cryst.*, **27,** 1129.
[21] Thisayukta, J., Nakayama, Y., Kawauchi, S., Takezoe, H., and Watanabe, J., 2000, *J. Amer. chem. Soc.*, **122,** 7441.
[22] Shen, D., Diele, S., Pelzl, G., Wirth, I., and Tschierske, C., 1999, *J. mater. Chem.*, **9,** 661.